Bacterial swarming reduces *Proteus mirabilis* and *Vibrio parahaemolyticus* cell stiffness and increases β-lactam susceptibility

George K. Auer[a], Piercen M. Oliver[b], Manohary Rajendram[b], Qing Yao[c,d], Grant J. Jensen[c, d], and Douglas B. Weibel[a,b,e*]

[a] Department of Biomedical Engineering, University of Wisconsin-Madison, Madison, WI, 53706
[b] Department of Biochemistry, University of Wisconsin-Madison, Madison, WI, 53706
[c] Division of Biology and Biological Engineering, California Institute of Technology, Pasadena, CA 91125
[d] Howard Hughes Medical Institute, California Institute of Technology, Pasadena, CA 91125
[e] Department of Chemistry, University of Wisconsin-Madison, Madison, WI, 53706

*** Author to whom correspondence should be addressed:**
Douglas B. Weibel
Department of Biochemistry
6424 Biochemical Sciences Building
440 Henry Mall
Phone: +1 (608) 890-1342
Fax: +1 (608) 265-0764
E-mail: douglas.weibel@wisc.edu

Classification: Biological Sciences; Microbiology

Keywords: bacterial swarming, bacterial cell mechanics; peptidoglycan; osmotic pressure; antibiotics

Abstract

Swarmer cells of the gram-negative pathogenic bacteria *Proteus mirabilis* and *Vibrio parahaemolyticus* become long (>10-100 μm) and multinucleate during their growth and motility on polymer surfaces. We demonstrate increasing cell length is accompanied by a large increase in flexibility. Using a microfluidic assay to measure single-cell mechanics, we identified large differences in swarmer cell stiffness of (bending rigidity of *P. mirabilis*, 9.6 x 10^{-22} N m^2; *V. parahaemolyticus*, 9.7 x 10^{-23} N m^2) compared to vegetative cells (1.4 x 10^{-20} N m^2 and 3.2 x 10^{-22} N m^2, respectively). The reduction in bending rigidity (~3-15 fold) was accompanied by a decrease in the average polysaccharide strand length of the peptidoglycan layer of the cell wall from 28-30 to 19-22 disaccharides. Atomic force microscopy revealed a reduction in *P. mirabilis* peptidoglycan thickness from 1.5 nm (vegetative) to 1.0 nm (swarmer) and electron cryotomography indicated changes in swarmer cell wall morphology. *P. mirabilis* and *V. parahaemolyticus* swarmer cells became increasingly sensitive to osmotic pressure and susceptible to cell wall-modifying antibiotics (compared to vegetative cells)—they were ~30% more likely to die after 3 h of treatment with minimum inhibitory concentrations of the β-lactams cephalexin and penicillin G. Long, flexible swarmer cells enables these pathogenic bacteria to form multicellular structures and promotes community motility. The adaptive cost of swarming is offset by a fitness cost in which cells are more susceptible to physical and chemical changes in their environment, thereby suggesting

58 the development of new chemotherapies for bacteria that leverage swarming for
59 survival.
60
61 **Significance Statement**
62 *Proteus mirabilis* and *Vibrio parahaemolyticus* are bacteria that infect humans. To adapt to
63 environmental changes, these bacteria alter their cell morphology and move collectively
64 to access new sources of nutrients in a process referred to as 'swarming'. We found that
65 a change in the composition and thickness of the peptidoglycan layer of the cell wall
66 makes swarmer cells of *P. mirabilis* and *V. parahaemolyticus* more flexible (i.e., reduced
67 cell stiffness) and increases their sensitivity to osmotic pressure and cell-wall targeting
68 antibiotics (e.g., β-lactams). These results highlight the importance of assessing the
69 extracellular environment in determining antibiotic doses and the use of β-lactams
70 antibiotics for treating infections caused by swarmer cells of *P. mirabilis* and *V.*
71 *parahaemolyticus*.
72 "\body"
73
74
75
76
77

Introduction

Bacteria have evolved a variety of mechanisms to adapt to their physical environment. For example, in response to fluctuating environmental conditions, changes in biochemistry and gene regulation can alter bacterial shape and increase cell fitness. Cell filamentation is a commonly observed change in bacterial cell shape (1, 2) and has been described as a mechanism that enables bacteria to evade predation by the innate immune system during host infections (1).

In close proximity to surfaces, many bacteria alter their morphology and leverage cell-cell physical contact to move collectively to access new sources of nutrients and growth factors (3, 4). Referred to as 'swarming', this process is common among motile bacteria, has been connected to bacterial pathogenesis and infections, and is an example of adaptive behavior (3, 4). Swarmer cells of *Salmonella enterica*, *Pseudomonas aeruginosa*, *Serratia marcescens*, and *Bacillus subtilis* have reduced susceptibility—compared to vegetative cells—to a variety of antibiotics that target protein translation, DNA transcription, and the bacterial cell membrane and cell wall (5-8). The specific biochemical and biophysical mechanisms underlying these observations are unknown.

Here, we describe physical changes in swarmer cells of the gram-negative pathogenic bacteria *Proteus mirabilis* and *Vibrio parahaemolyticus* that increase their susceptibility to cell wall-targeting clinical antibiotics. We found that large changes in the length of *P. mirabilis* and *V. parahaemolyticus* swarmer cells are accompanied by an

increase in flexibility (i.e., a reduction in cell stiffness) that enables long cells to pack together tightly and form cell-cell interactions; these interactions have been demonstrated previously to promote surface motility (9). Using biophysical, biochemical, and structural techniques, we quantified changes in the structure and composition of the *P. mirabilis* and *V. parahaemolyticus* cell wall in swarmer and vegetative cells and characterized their susceptibility to osmotic changes and cell wall-modifying antibiotics. Our results indicate that morphological changes that enable these bacteria to adapt to new physical environments come at a significant fitness cost: cells become more susceptible to changes in their chemical environment. These results predict cell wall-modifying antibiotics should deter infections of *P. mirabilis* and *V. parahaemolyticus* in which swarming is implicated (e.g., in urinary tract infections).

Results

The bending rigidity of *P. mirabilis* and *V. parahaemolyticus* cells decreases during swarming. During surface motility, *P. mirabilis* and *V. parahaemolyticus* cells grow into swarmers that are characteristically long (10-100 μm) and present a high surface density of flagella that enables them to translate through viscous environments (3, 10). We found that these swarmer cells display an unusual phenotype that is rarely observed among gram-negative bacteria: cells become remarkably flexible and their shape is dynamically altered by adjacent cell motion and collisions (Fig. 1). The ability of *P.*

118 *mirabilis* swarmer cells to form cell-cell contacts plays a role in their cooperative motility
119 (10), leading us to hypothesize that increasing flexibility enables these long cells to
120 optimize packing into multicellular structures that move cooperatively across surfaces.
121 Bacterial cell mechanics is generally attributed to the peptidoglycan (PG) layer of the
122 cell wall, which has a thickness of ~3-50 nm and surrounds the cytoplasmic membrane
123 (11). Very little is known about mechanical regulation in bacteria (12-17) and we are
124 unaware of studies connecting swarming to changes in cell mechanics. We quantified
125 changes in swarmer-cell stiffness using cell-bending assays in a reloadable,
126 poly(dimethylsiloxane) microfluidic system (Fig. 2 and S1) that is related to a method
127 developed previously (18). In bending assays, we applied a shear fluid force to multiple
128 filamentous cells, resulting in horizontal deflection of their cell tips (Fig. 2); fitting the
129 deflection data to a mechanical model provided us with a value of the (flexural)
130 bending rigidity of cells (Fig. S2). Introducing a reloadable mechanism enabled us to
131 perform rapid bending measurements of *P. mirabilis* and *V. parahaemolyticus* swarmer
132 cells after isolating them from swarm plates. As a point of comparison, we filamented
133 vegetative cells of *P. mirabilis* and *V. parahaemolyticus* using aztreonam—an inhibitor of
134 the division specific transpeptidase PBP3—to match the length of swarmer cells and
135 compared their bending rigidity values to swarmer cells. As a control, we measured the
136 bending rigidity of cells of *Escherichia coli* strain MG1655 that we filamented using
137 aztreonam, and determined the value to be 9.7×10^{-23} N m^2 (Fig. 3); using a value for the

thickness of the PG of 4-nm (19) yields a Young's modulus of 26 MPa, which is close to values that have been reported previously (12, 18).

We used bending rigidity as a parameter to quantify *P. mirabilis* and *V. parahaemolyticus* cell stiffness rather than Young's modulus, as the latter metric of the mechanical properties of materials is dependent on cell-wall thickness, which we hypothesized may change during swarming (described below). We found a substantial decrease in the bending rigidity of swarmer cells of both *P. mirabilis* (~15-fold) and *V. parahaemolyticus* (3-fold) compared to their vegetative cell counterparts (Fig. 3), which is consistent with our observations of the shape and behavior of these cells during swarming on surfaces. *V. parahaemolyticus* vegetative cells were remarkably flexible: ~134-fold more so than *E. coli* cells and ~3-fold more than *P. mirabilis* swarmer cells (Fig. 3).

To confirm that using aztreonam to inhibit PBP3 and produce filamentous cells did not change the cross-linking density of PG at the division plane and alter cell mechanics, we compared bending rigidity values of cells treated with aztreonam and cells filamented by overexpressing SulA, a protein that prevents polymerization of the division protein FtsZ and blocks cell division. Both mechanisms of filamenting *E.* coli cells produced similar bending rigidity values: 4.0×10^{-20} N m^2 (SulA) and 4.1×10^{-20} N m^2 (aztreonam) (Fig. S4*A*). To account for the high surface density of flagella on swarmer cells, which may contribute to cell drag in fluid flow and bias measurements,

158 we performed bending rigidity measurements (Fig. S4*B*) on two K-12-derived strains of
159 *E. coli* with substantially different flagella densities (Fig. S4*C*) and observed no
160 appreciable change in values (bending rigidity of 4.0×10^{-20} N m^2 at high flagella density
161 and 4.1×10^{-23} N m^2 at low flagella density; Fig. S4*B*).

162 Overexpressing FlhDC—the heterohexameric activator that is important for
163 swarming—in vegetative cells growing in liquid produces a phenotype that replicates
164 many of the characteristics of swarmer cells, including increased cell length and flagella
165 density (20). The relationship between FlhDC and cell mechanics has not yet been
166 reported. To test whether FlhDC is connected to changes in swarmer cell stiffness, we
167 overexpressed the protein from the plasmid-encoded genes *pflhDC* in filamentous cells
168 of *P. mirabilis* and measured their bending rigidity. We detected a ~1.5-fold difference in
169 bending rigidity between wildtype (1.4×10^{-20} N m^2) and *pflhDC*-containing *P. mirabilis*
170 vegetative cells (9.2×10^{-21} N m^2), and no difference compared to *pflhDC*-containing *P.*
171 *mirabilis* swarmer cells (Fig. 3). These results indicate that FlhDC overexpression during
172 swarming contributes a small amount to the mechanical phenotype of swarming cells,
173 however the majority of the mechanical changes we observe arises from PG alterations
174 through another regulatory pathway.

175

176 **Changes in PG composition of *P. mirabilis* and *V. parahaemolyticus* swarmer cells.**
177 PG consists of the disaccharide building block β-(1,4)-N-acetylmuramic acid/N-acetyl-

178 glucosamine (MurNAc-GlcNAc) in which a pentapeptide is attached to each 3′-OH
179 group on MurNAc. Cross-linking between adjacent pentapeptides creates a mesh-like
180 polymeric layer, and altering its structure and composition affects cell-mechanical
181 properties (14, 15). To determine whether the PG composition of *P. mirabilis* and *V.*
182 *parahaemolyticus* cells changes during swarming, we isolated PG sacculi from vegetative
183 and swarmer cells and used ultra performance liquid chromatography-mass
184 spectrometry (UPLC-MS) to quantify its chemical composition (Fig. S*5*). As the PG
185 composition of *V. parahaemolyticus* has not yet been reported, we characterized its
186 muropeptide stem peptide using UPLC-MS/MS (Fig. S*6* and Table S1). Similar to *E. coli*
187 (21) and *P. mirabilis* (22), *V. parahaemolyticus* has a PG structure that is conserved across
188 other gram-negative bacteria, in which the peptide stem consists of L-Ala-D-Glu-*meso*-
189 diaminopimelic acid (*meso*-DAP)-D-Ala-D-Ala (Fig. S6).
190 Compared to vegetative cells, *P. mirabilis* swarmer cells contained fewer
191 monomers (MurNAc-GlcNAc), more dimers, and more anhydrous-containing
192 saccharides, which are found at the terminating end of glycan polymers (Fig. 4*A*) (11).
193 We detected no differences in the relative abundance of trimers between swarmer and
194 vegetative cells of *P. mirabilis* (Fig. 4*A*). The increase in anhydrous-containing
195 saccharides that we observed in *P. mirabilis* swarmer cells was correlated with a
196 decrease in polysaccharide length (Fig. 4*B*; the values plotted reflect the number of
197 MurNAc-GlcNAc dimers). A similar increase in anhydrous-containing saccharides and

198 decreased length of polysaccharides occurred in *V. parahaemolyticus* swarmer cells (Fig.
199 4*A, B*). We found no change in cross-linking density between vegetative and swarmer
200 cells of either *P. mirabilis or V. parahaemolyticus* (Fig. 4*C*).
201
202 **Swarmer cells have a reduced PG thickness and display membrane defects.** Changes
203 in the thickness of the PG layer and structure of the cell envelope may also explain the
204 observed decrease in swarmer cell stiffness. To identify changes in PG thickness of
205 swarmer cells, we isolated the intact layer of PG (i.e., sacculi) from *P. mirabilis*
206 vegetative and swarmer cells and measured the thickness of dried sacculi using
207 tapping-mode atomic force microscopy (AFM) (Fig. 5*A*). Differences in the nanoscopic
208 appearance of the sacculi of different cells were not observed by AFM (Fig. S7). The
209 thickness of isolated, dry *P. mirabilis* swarmer cell sacculi (1.0 ± 0.2 nm) was reduced
210 ~1.5-fold compared to vegetative cells (1.5 ± 0.2 nm) (Fig. 5*A*). *V. parahaemolyticus*
211 swarmer cells (0.6 ± 0.1 nm) exhibited a similar ~1.2-fold decrease in thickness
212 compared to vegetative cells (0.8 ± 0.2 nm). Earlier AFM measurements of isolated
213 sacculi indicated that dehydration reduced the thickness of *Escherichia coli* PG by ~2x,
214 which we used to estimate the dimensions of hydrated PG from *P. mirabilis* (3.1 and 2.1
215 nm for vegetative and swarmer cells, respectively) and *V. parahaemolyticus* (1.7 and 1.4
216 nm, respectively) (23). A comparison of PG thickness and cell bending rigidity

suggested that the relationship between these data is approximately exponential (R^2=0.9874) (Fig. 5*B*).

A caveat with conversions between dried and hydrated values is that they will be most accurate for PG that best mimics the structure and composition (e.g., crosslinking and polysaccharide composition) of the reference material: *E. coli* PG. Alterations in the polysaccharide length of PG from *P. mirabilis* and *V. parahaemolyticus* may be more elastic and stretch out during drying, thereby appearing to have a thickness that is reduced compared to *E. coli* PG. Our control measurements on isolated, dry *E. coli* sacculi yielded a thickness of 2.0 nm, which varies from the value of 3.0 nm published by Yao et al. using the same technique (23). A difference of ~30% between these *E. coli* measurements may arise for several reasons, including: variations in physical conditions that can impact AFM measurements, improvement in the resolution of AFMs, and/or the precision of fitting force curves.

The relatively low variability in the values we measured for isolated sacculi from *P. mirabilis* and *V. parahaemolyticus* cells (~16-25%) demonstrated a consistent reduction in PG thickness for swarmer cells, suggesting that our measurements are sufficient for comparing PG from vegetative and swarming cells, and demonstrating a connection between PG and changes in cell mechanics. In contrast, the variability in AFM measurements and analysis makes us less comfortable comparing absolute values of PG thickness to those reported for bacteria in other papers.

237 To complement AFM measurements, we sought to measure the thickness of
238 native PG using electron cryotomography (ECT) on intact vegetative and swarmer cells
239 (Figs. 5*C*,*D*, S8, and S9). Although we were unable to resolve the thickness of native PG,
240 sub-tomogram-averaged ECT volumes of the *P. mirabilis* cell wall (Fig. 5*C*) indicated
241 that the distance between the inner and outer membrane of swarmer cells was smaller
242 than in vegetative cells (Figs. *5*C,*D*). *P. mirabilis* vegetative cells had a characteristically
243 smooth membrane (Fig. S8*A*,*B*) that was similar to the presentation of the membrane
244 found along the lateral, cylindrical walls of swarmer cells (Fig. S8*C*,*D*). In contrast, the
245 polar regions of both *P. mirabilis* and *V. parahaemolyticus* swarmer cells had an
246 undulating outer membrane suggestive of an altered structure (Fig. S8*E*,*F* and *S9D-F*),
247 and *V. parahaemolyticus* cells had significant defects in their cell-envelope, including,
248 membrane budding, vesicle formation, and ruptured cell walls (Fig. S9*D-F*).
249
250 ***P. mirabilis* and *V. parahaemolyticus* swarmer cells are more sensitive to osmotic**
251 **stress than vegetative cells.** To complement cell stiffness measurements, we
252 investigated the mechanics of swarmer cells and filamented vegetative cells by
253 measuring their changes in length and volume in response to changes in osmotic
254 pressure, which will cause cells to shrink cells (in H_2O) and swell (in a NaCl solution)
255 (Fig. S10). We filamented *P. mirabilis*, *V. parahaemolyticus*, and control *E. coli* cells using
256 aztreonam to create a range of cell lengths that matched the lengths of *P. mirabilis* and *V.*

257 *parahaemolyticus* swarmer cells. We expected that low values of bending rigidity and
258 compositional and structural changes in PG would cause swarmer cells to elongate in
259 response to changes in osmotic pressure (in comparison to filamented, vegetative cells).
260 We found that *P. mirabilis* and *V. parahaemolyticus* swarmer cell extension in response to
261 osmotic shock was significantly larger than filamented, vegetative cells (Fig. 6). To
262 circumvent the cellular production of osmolytes to protect cells from large changes in
263 osmotic pressure during shock (typically produced within 1 min) (24), we used a
264 microfluidic device to rapidly switch between H_2O and a NaCl solution and measured
265 changes in cell length before cells adapted (Fig. S10).
266 Osmotic shifts produced small changes in the length (Fig. 6*A*) and width (Fig. 6*B*)
267 of vegetative filamented *P. mirabilis* cells compared to *E. coli* cells (Figs. 6*A*,*B*). In
268 contrast, *V. parahaemolyticus* vegetative cells substantially increased in cell length (Fig.
269 6C) compared to *E. coli* cells, with no observable change in cell width (Fig. 6*D*). In
270 response to osmotic upshifts (i.e., transitioning from H_2O to NaCl), *P. mirabilis* and *V.*
271 *parahaemolyticus* swarmer cells dramatically increased in cell length (Figs. 6*A*, *C*) (and to
272 a lesser extent, cell width for *P. mirabilis* but not for *V. parahaemolyticus*; Figs. 6*B*, *D*)
273 compared to vegetative cells. These results suggest that changes in *P. mirabilis* and *V.*
274 *parahaemolyticus* swarmer cell mechanics make them more responsive to osmotic
275 changes.
276

Increased susceptibility of *P. mirabilis* and *V. parahaemolyticus* swarmers to the cell wall-targeting antibiotics. Although swarming colonies of bacteria display resistance to many antibiotics (5), our experiments suggest *P. mirabilis* and *V. parahaemolyticus* swarmers may have increased susceptibility to cell wall-targeting antibiotics that further alter PG structure, composition, and properties. To determine the sensitivity of *P. mirabilis* and *V. parahaemolyticus* swarmers to the cell wall-targeting antibiotics cephalexin (inhibits PBP3 and 4) (25) and penicillin G (inhibits PBP3, 4, and 6), we measured swarmer single-cell growth in the presence of the minimum inhibitory concentration (MIC) of antibiotics in a microfluidic device (Figs. S11) for 3 h. The time scale of this experiment was chosen based on two previous reports: 1) treating cells with cephalexin for 3 h was sufficient to kill ~100% of a population of *E. coli* cells (26); and 2) ~2 h of cephalexin treatment was sufficient to observe cell lysis of *E. coli* cells measured by single cell growth (27).

Using a microfluidic device enabled us to supply cells with a source of continuously replenished fresh growth media to ensure exponential cell growth and a constant concentration of antibiotics. We found that the survival of *P. mirabilis* (66%) and *V. parahaemolyticus* (64%) vegetative cells treated with 1X MIC of cephalexin was slightly higher than *E. coli* cells (55%) (Figs. 7*A*, S12). Treating *P. mirabilis* and *V. parahaemolyticus* swarmer cells with 1X MIC of cephalexin reduced survival to 37% and 19%, respectively (Figs. 7*A*, S12), indicating their increased susceptibility. Rates of cell

297 survival in the presence of penicillin G were similar to the use of cephelexin (Fig. 7*A*).
298 We characterized dead cells using microscopy to measure membrane blebbing, cell
299 lysis, and changes in the refractive index of cells.

300 Cell wall-targeting antibiotics are most effective against actively growing cells
301 (28, 29) and therefore increases in growth rate will reduce cell survival. To determine
302 whether a growth rate phenotype explains our observations, we normalized data for
303 cell length, and were unable to detect a change in the growth rate of swarmer cells
304 when they were treated with these two antibiotics (Fig. S13). We measured the mean
305 survival time of cells (the amount of time elapsed after treatment with drugs before cell
306 death) for *P. mirabilis* and *V. parahaemolyticus* swarmer cells treated with cephalexin and
307 penicillin G (Fig. 7*B*) and found that the survival time for these swarmer cells was lower
308 than that for vegetative cells (Fig. 7*B*), which is consistent with alterations in the PG.

309

310 **Discussion**

311 *P. mirabilis* is commonly associated with complicated urinary tract infections and
312 increased mortality in cases of bacteremia (30). Swarming is hypothesized to enable *P.*
313 *mirabilis* cell movement from the ureter to the kidney; in support of this hypothesis,
314 swarming deficient mutants have lower rates of host infection (31). We found that
315 during swarming, *P. mirabilis* and *V. parahaemolyticus* cells become more flexible due to
316 changes in PG composition and cell wall structure. Presumably this phenotype conveys

317 an adaptive advantage for cells that we hypothesize improves community motility by
318 enabling long swarmer cells to form cell-cell contacts that are demonstrated to enhance
319 motility. The adaptive advantage of swarming in *P. mirabilis* and *V. parahaemolyticus* is
320 offset by a decrease in their fitness, as cells become more sensitive to osmotic changes
321 and cell wall-targeting antibiotics, thereby creating an "Achilles heal" for targeting this
322 phenotype in infectious diseases. This study highlights the plasticity of bacteria (1), the
323 need for devising tests for treatments that measure efficacy against cells in a
324 physiological state relevant to specific infections, and re-considering the use of cell wall-
325 targeting antibiotics for treating UTIs in which *P. mirabilis* may be present.
326
327 **Materials and Methods**
328 **Bacterial strains and cell culture.** *P. mirabilis* strain HI4320, *V. parahaemolyticus* LM5674,
329 *Escherichia coli* MG1655 (CGSC #6300), and plasmids *pflhDC* (10) and *psulA*(18) were
330 used for experiments used in this paper. *P. mirabilis* was grown in PLB nutrient medium
331 consisting of 1% peptone (weight/volume), 0.5% yeast extract (w/v), and 1% NaCl (w/v).
332 *V. parahaemolyticus* was grown in nutrient medium (HI medium) consisting of 2.5%
333 heart infusion (w/v) and 2.5% NaCl (w/v). *E. coli* was grown in lysogeny broth (LB)
334 consisting of 1% tryptone (w/v), 0.5% yeast extract (w/v), and 1% NaCl (w/v). All strains
335 were grown at 30 °C with shaking at 200 rpm. Additional data and methods are
336 described in Supplementary Information.

Acknowledgements. We thank Linda McCarter for *V. parahaemolyticus* LM5674, Suckjoon Jun for the *psulA* plasmid, Cameron Scarlett and Molly Pellitteri-Hahn for mass spectrometry support, and Julie Last for technical assistance with AFM measurements. This research was supported by NIH grant 1DP2OD008735-01, National Science Foundation grant DMR-1121288, a Mao Wisconsin Distinguished Graduate Fellowship (to M.R.), and an NSF postdoctoral fellowship (#1202622 to P.M.O), and the Howard Hughes Medical Institute.

References

1. Justice SS, Hunstad DA, Cegelski L, & Hultgren SJ (2008) Morphological plasticity as a bacterial survival strategy. *Nat Rev Microbiol* 6(2):162-168.
2. Rajendram M, *et al.* (2015) Anionic phospholipids stabilize RecA filament bundles in Escherichia coli. *Mol Cell* 60(3):374-384.
3. Copeland MF & Weibel DB (2009) Bacterial Swarming: A Model System for Studying Dynamic Self-assembly. *Soft Matter* 5(6):1174-1187.
4. Kearns DB (2010) A field guide to bacterial swarming motility. *Nat Rev Microbiol* 8(9):634-644.
5. Butler MT, Wang Q, & Harshey RM (2010) Cell density and mobility protect swarming bacteria against antibiotics. *Proc Natl Acad Sci U S A* 107(8):3776-3781.
6. Kim W, Killam T, Sood V, & Surette MG (2003) Swarm-cell differentiation in Salmonella enterica serovar typhimurium results in elevated resistance to multiple antibiotics. *J Bacteriol* 185(10):3111-3117.
7. Overhage J, Bains M, Brazas MD, & Hancock RE (2008) Swarming of Pseudomonas aeruginosa is a complex adaptation leading to increased production of virulence factors and antibiotic resistance. *J Bacteriol* 190(8):2671-2679.
8. Lai S, Tremblay J, & Deziel E (2009) Swarming motility: a multicellular behaviour conferring antimicrobial resistance. *Environ Microbiol* 11(1):126-136.
9. Hay NA, Tipper DJ, Gygi D, & Hughes C (1999) A novel membrane protein influencing cell shape and multicellular swarming of Proteus mirabilis. *J Bacteriol* 181(7):2008-2016.
10. Tuson HH, Copeland MF, Carey S, Sacotte R, & Weibel DB (2013) Flagellum density regulates Proteus mirabilis swarmer cell motility in viscous environments. *J Bacteriol* 195(2):368-377.
11. Vollmer W & Seligman SJ (2010) Architecture of peptidoglycan: more data and more models. *Trends Microbiol* 18(2):59-66.
12. Wang S, Arellano-Santoyo H, Combs PA, & Shaevitz JW (2010) Actin-like cytoskeleton filaments contribute to cell mechanics in bacteria. *Proc Natl Acad Sci U S A* 107(20):9182-9185.
13. Tuson HH, *et al.* (2012) Measuring the stiffness of bacterial cells from growth rates in hydrogels of tunable elasticity. *Mol Microbiol* 84(5):874-891.
14. Wheeler R, *et al.* (2015) Bacterial Cell Enlargement Requires Control of Cell Wall Stiffness Mediated by Peptidoglycan Hydrolases. *Mbio* 6(4):e00660.
15. Loskill P, *et al.* (2014) Reduction of the peptidoglycan crosslinking causes a decrease in stiffness of the Staphylococcus aureus cell envelope. *Biophys J* 107(5):1082-1089.

16. Auer GK, *et al.* (2016) Mechanical Genomics Identifies Diverse Modulators of Bacterial Cell Stiffness. *Cell Syst* 2(6):402-411.
17. Auer GK & Weibel DB (2017) Bacterial Cell Mechanics. *Biochemistry-Us* 56(29):3710-3724.
18. Amir A, Babaeipour F, McIntosh DB, Nelson DR, & Jun S (2014) Bending forces plastically deform growing bacterial cell walls. *Proc Natl Acad Sci U S A* 111(16):5778-5783.
19. Gan L, Chen S, & Jensen GJ (2008) Molecular organization of Gram-negative peptidoglycan. *Proc Natl Acad Sci U S A* 105(48):18953-18957.
20. Patrick JE & Kearns DB (2012) Swarming motility and the control of master regulators of flagellar biosynthesis. *Mol Microbiol* 83(1):14-23.
21. Desmarais SM, *et al.* (2015) High-throughput, highly sensitive analyses of bacterial morphogenesis using ultra performance liquid chromatography. *J Biol Chem* 290(52):31090-31100.
22. Strating H, Vandenende C, & Clarke AJ (2012) Changes in peptidoglycan structure and metabolism during differentiation of Proteus mirabilis into swarmer cells. *Can J Microbiol* 58(10):1183-1194.
23. Yao X, Jericho M, Pink D, & Beveridge T (1999) Thickness and elasticity of gram-negative murein sacculi measured by atomic force microscopy. *J Bacteriol* 181(22):6865-6875.
24. McLaggan D, Naprstek J, Buurman ET, & Epstein W (1994) Interdependence of K+ and glutamate accumulation during osmotic adaptation of Escherichia coli. *J Biol Chem* 269(3):1911-1917.
25. Eberhardt C, Kuerschner L, & Weiss DS (2003) Probing the catalytic activity of a cell division-specific transpeptidase in vivo with beta-lactams. *J Bacteriol* 185(13):3726-3734.
26. Chung HS, *et al.* (2009) Rapid beta-lactam-induced lysis requires successful assembly of the cell division machinery. *Proc Natl Acad Sci U S A* 106(51):21872-21877.
27. Yao Z, Kahne D, & Kishony R (2012) Distinct single-cell morphological dynamics under beta-lactam antibiotics. *Mol Cell* 48(5):705-712.
28. Tuomanen E, Cozens R, Tosch W, Zak O, & Tomasz A (1986) The Rate of Killing of Escherichia-Coli by Beta-Lactam Antibiotics Is Strictly Proportional to the Rate of Bacterial-Growth. *J Gen Microbiol* 132:1297-1304.
29. Spoering AL & Lewis K (2001) Biofilms and planktonic cells of Pseudomonas aeruginosa have similar resistance to killing by antimicrobials. *J Bacteriol* 183(23):6746-6751.
30. Chen CY, *et al.* (2012) Proteus mirabilis urinary tract infection and bacteremia: risk factors, clinical presentation, and outcomes. *J Microbiol Immunol Infect* 45(3):228-236.

435 31. Burall LS*, et al.* (2004) Proteus mirabilis genes that contribute to pathogenesis of
436 urinary tract infection: Identification of 25 signature-tagged mutants attenuated
437 at least 100-fold. *Infect Immun* 72(5):2922-2938.
438

439

440

441

FIGURES

Fig. 1. Images demonstrating the flexibility of *P. mirabilis* and *V. parahaemolyticus* swarmer cells. (*A*) Time-series of *P. mirabilis* swarmer cells in a colony actively moving across the surface of a 1.5% agarose gel. A representative cell, false colored green, has a generally straight shape at t=0 s and is bent in half at t=0.98 s. Most of the cells in this frame are bending during this imaging sequence. (*B*) A time-series of *V. parahaemolyticus* swarmer cells in a colony actively moving across the surface of a 1.4% agarose gel. A representative cell (false colored purple) has a generally straight shape at t=0 s and is bent in half at t=4.02 s.

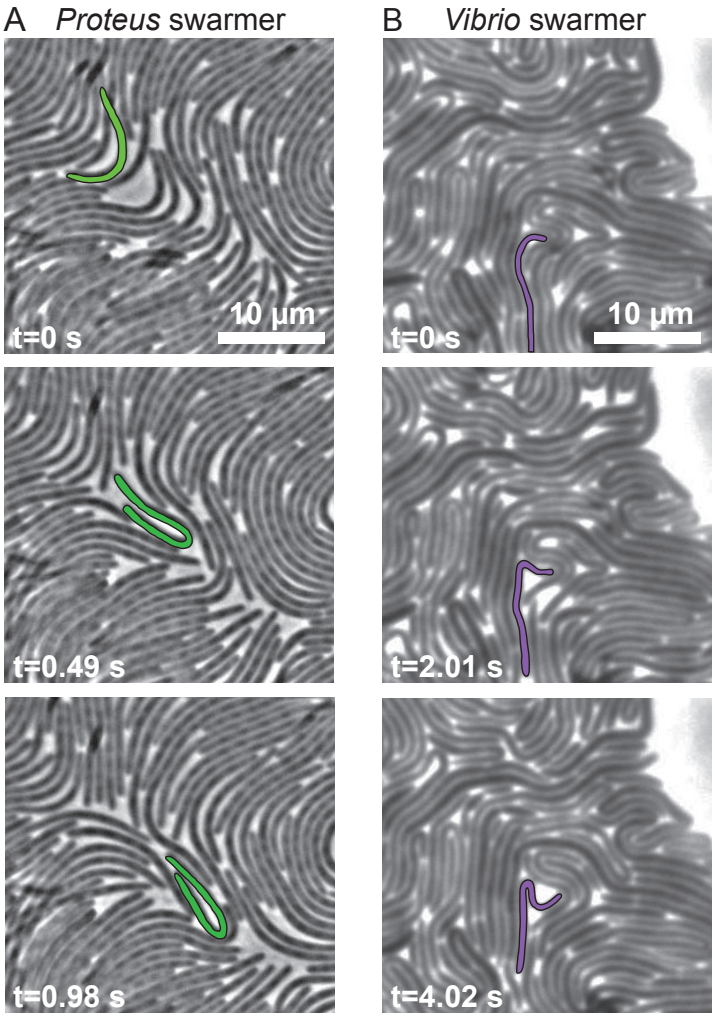

Fig. 1

Fig. 2. Using a reloadable microfluidic-based assay to determine bacterial cell stiffness. (*A*) Schematic of the microfluidic channel used to apply a user-defined shear force to bend filamentous or swarmer cells. Single-sided green arrows depict the flow of fluid through the central channel; the parabolic flow profile of the fluid is shown. Double-sided green arrows indicate the vacuum chamber used to load cells into side channels and to empty the device. (*B*) Cartoon of a flexible bacterium (left) and a stiff bacterium (right) under flow force (V_{flow}). x_{max} indicates the deflection of cells in the flow; $2r$ = cell diameter; L = cell length in contact with the flow force. (*C*) Representative images of filamentous cells of *P. mirabilis* in no flow (left) and flow (right) conditions (top) and *P. mirabilis* swarmers (bottom). Purple dashed lines indicate the position of a cell tip under no flow conditions and black dashed lines illustrate the position after flow is applied using a gravity-fed mechanism. The arrow indicates the direction of fluid flow in the channel.

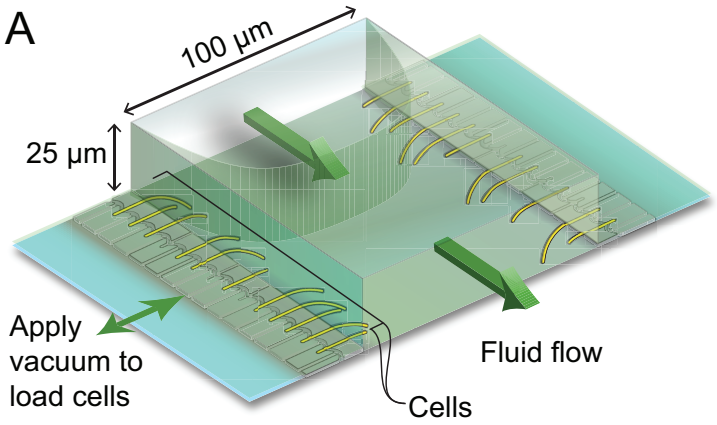

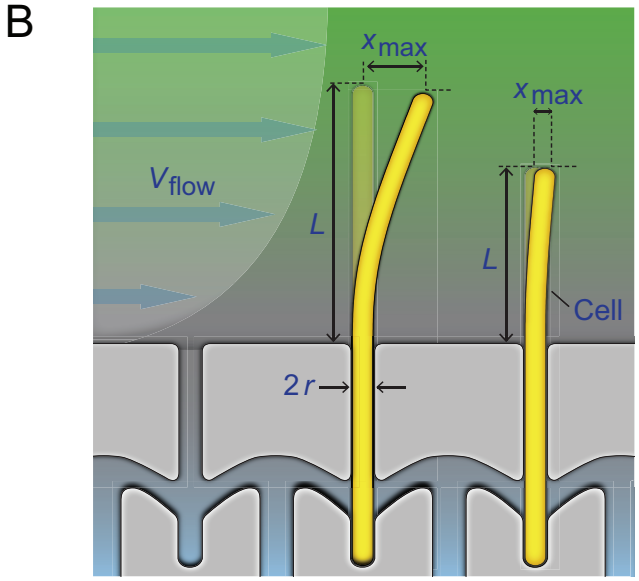

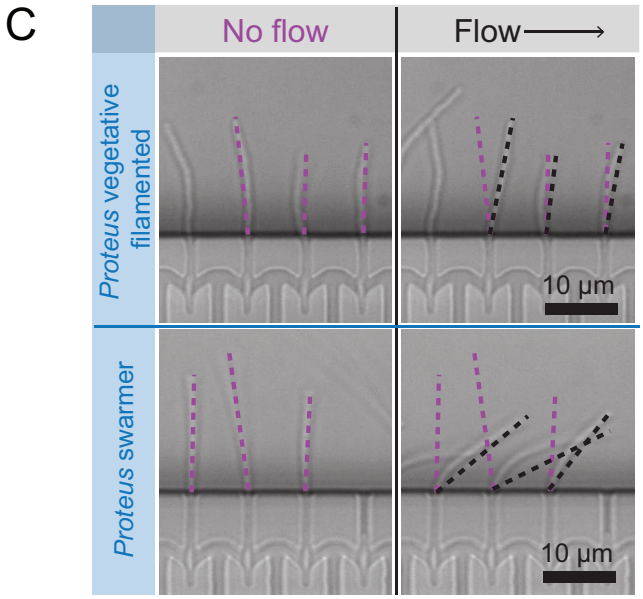

476 **Fig 2.**

Fig. 3. *P. mirabilis* and *V. parahaemolyticus* swarmer cells have a lower bending rigidity than vegetative cells. We measured the bending rigidity of *P. mirabilis* and *V. parahaemolyticus* swarmer cells and filamentous vegetative cells in a microfluidic flow assay and included measurements of vegetative *E. coli* cells. *P. mirabilis* swarmers exhibited 15-fold lower bending rigidity than vegetative cells; *V. parahaemolyticus* swarmers were 3-fold less rigid than vegetative cells. Overexpression of FlhDC (from the plasmid-encoded *pflhDC*) had little effect on the stiffness of *P. mirabilis* vegetative and swarmer cells. Error bars represent the 95% confidence interval of a fit to data. $n >$ 100 cells, from at least 3 independent experiments.

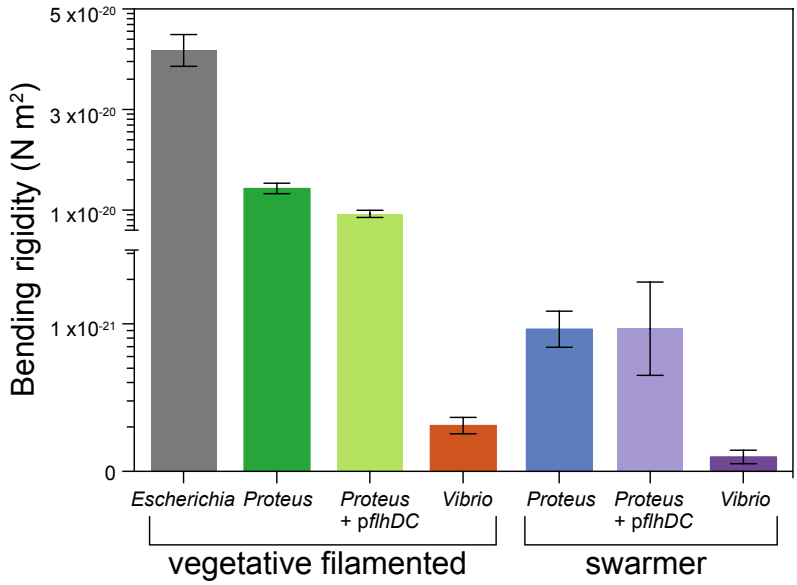

Fig 3.

Fig. 4. Alterations in the PG muropeptide composition of *P. mirabilis* and *V. parahaemolyticus* swarmer cells. (*A*) UPLC-MS data reveal that the muropeptide composition of *P. mirabilis* and *V. parahaemolyticus* vegetative and swarmer cells differs slightly in the abundance of monomer, dimer, and anhydrous-terminated saccharides. (*B*) We observed a relative increase in the amount of anhydrous-containing saccharides in swarmers consistent with a decrease in polysaccharide strand length. (*C*) There was no change in PG cross-linking of *P. mirabilis* and *V. parahaemolyticus* vegetative and swarmer cells, although *V. parahaemolyticus* does display a lower level of cross-linking. *n* = 3 biological replicates. Error bars represent the standard deviation of the mean. For (*A-C*), significance was determined via two-way analysis of variance: *P ≤ 0.05, **P ≤ 0.01, ***P ≤ 0.001, ****P ≤ 0.0001, ns = not significant (P > 0.05).

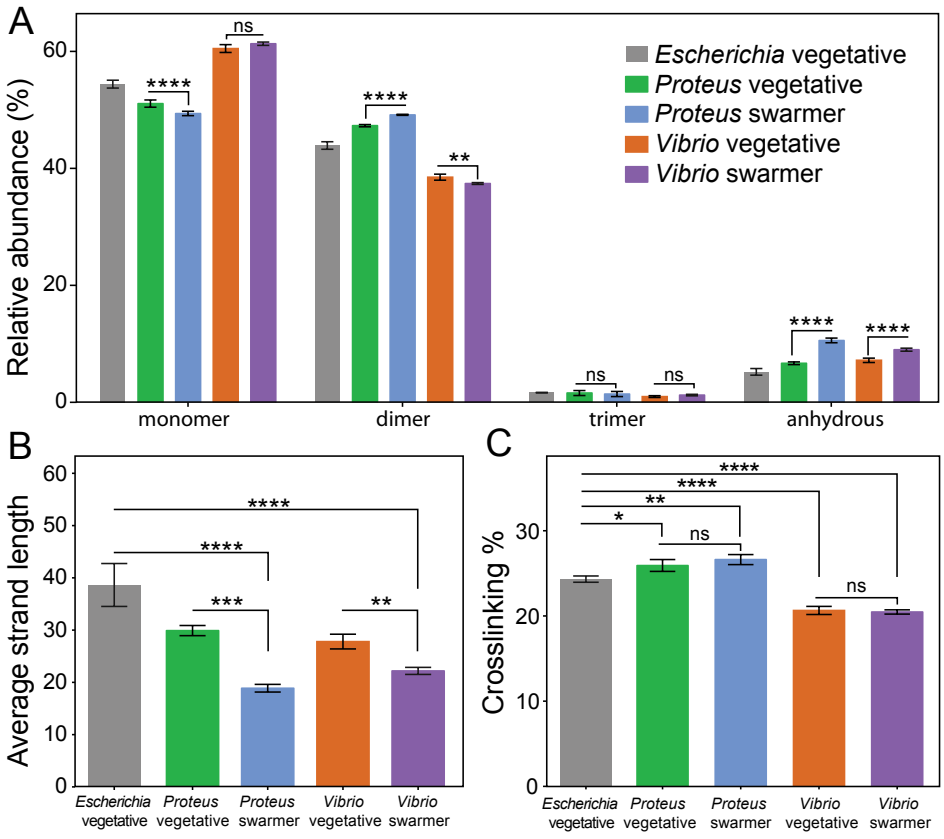

Fig 4.

Fig. 5. AFM reveals the PG layer of *P. mirabilis* and *V. parahaemolyticus* swarmer cells is thinner than in vegetative cells and ECT demonstrates a reduced membrane-to-membrane distance. (*A*) Sacculi were isolated from cells, dried, and imaged by AFM. The thickness of swarmer cell PG was reduced compared to vegetative cells. We analyzed >65 vegetative cells of *E. coli*, *P. mirabilis*, and *V. parahaemolyticus*, >65 *P. mirabilis* swarmer cells, and 7 *V. parahaemolyticus* swarmer cells. Error bars represent the standard deviation of the mean. (*B*) Bending rigidity and cell wall thickness display an approximately exponential relationship (R^2=0.9874). (*C*) Sub-tomogram-averaged ECT volume images of the *P. mirabilis* vegetative (left) and swarmer (right) cell wall. Two central slices of sub-tomogram average volume images with normalized image densities are shown. Yellow dashed line indicates the orientation used for gray-value measurements. ES, extracellular space; OM, outer membrane; PG, peptidoglycan; IM, inner membrane; CP, cytoplasm. (*D*) The density profile of sub-tomogram-averaged ECT volume images reveals a reduced membrane-to-membrane distance in swarmer cells. The vertical axis is the normalized gray value with the darkest value equal to 0 and the lightest value equal to 1. The red dashed line denotes the average gray value of the extracellular space and serves as a reference for the background; the blue shaded area indicates the thickness of the putative PG layer.

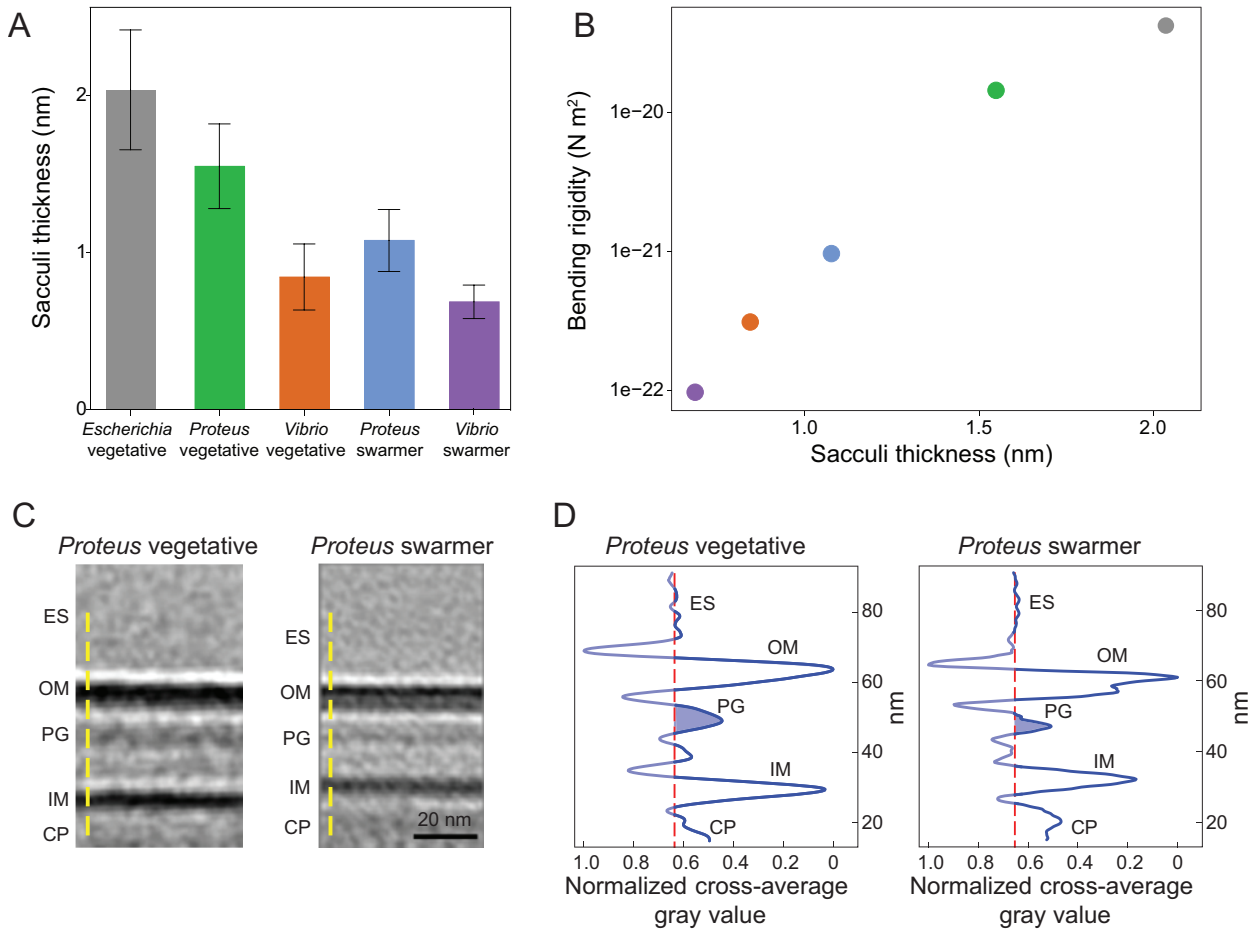

Fig 5.

557 **Fig. 6.** Swarmer cells increase in cell extension during osmotic shock. We calculated Δ*L*
558 as (cell length in water – cell length in 1 M NaCl) and performed a similar calculation
559 for Δ*W*, substituting cell width. Cell length indicates length prior to osmotic shock. We
560 filamented all vegetative cells using aztreonam to grow them to lengths that were
561 comparable with *P. mirabilis* and *V. parahaemolyticus* swarmers. Lines indicate linear fits
562 to single-cell measurements (circles) of $n > 100$ cells from at least 3 independent
563 experiments. (*A*) *P. mirabilis* swarmer cells have an increase in extension (Δ*L*) under
564 osmotic shock compared to *E. coli* and *P. mirabilis* vegetative cells. (*B*) *V. parahaemolyticus*
565 vegetative and swarmer cells have an increase in extension (Δ*L*) under osmotic shock
566 compared to *E. coli*. (*C*) *P. mirabilis* swarmer cells have an increase in Δ*W* compared to *E.*
567 *coli*; *P. mirabilis* vegetative cells display a slight decrease in width and increased cell
568 length. (*D*) There was no observable change in Δ*W* of *V. parahaemolyticus* swarmer and
569 vegetative cells.
570

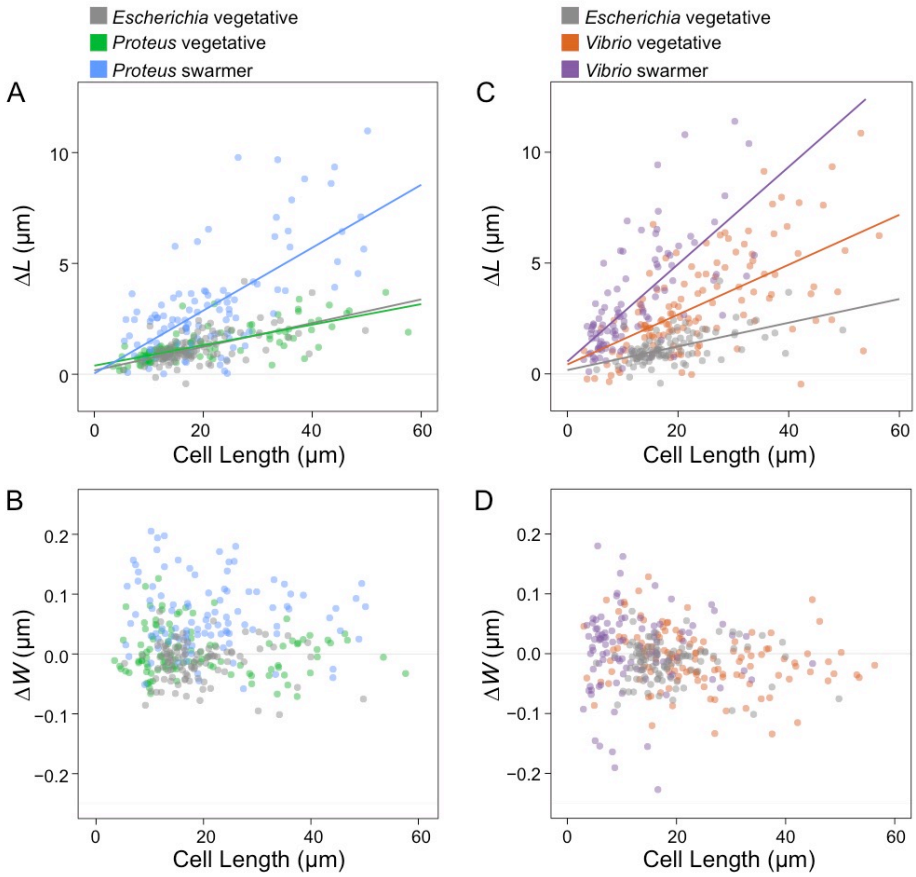

Fig 6.

580 **Fig. 7.** Swarmer cells are more susceptible to antibiotics that target the cell wall than are
581 vegetative cells. (*A*) Survival of cells treated with 1X MIC of cephalexin after 3 h of
582 incubation. We define percent survival as (cell count$_{\text{no lysis}}$ / cell count$_{\text{total}}$) x 100. *P.*
583 *mirabilis* and *V. parahaemolyticus* swarmer cells exhibit decreased levels (~30%) of
584 survival compared to vegetative cells; $n \geq 90$ cells from at least two independent
585 experiments. A similar decrease occurred when *P. mirabilis* was treated with penicillin
586 G; $n \geq 77$ cells from at least two independent experiments). Error bars represent the
587 standard deviation of the mean. (*B*) After exposure to cephalexin or penicillin G, the
588 survival time of *P. mirabilis* and *V. parahaemolyticus* swarmers was 2~3 fold lower than
589 for vegetative cells. Survival time was determined for ≥ 49 cells that lysed from at least 2
590 independent experiments. Significance in *A-B* was determined two-tailed t-test: *P ≤
591 0.05, **P ≤ 0.01, ****P ≤ 0.0001.
592

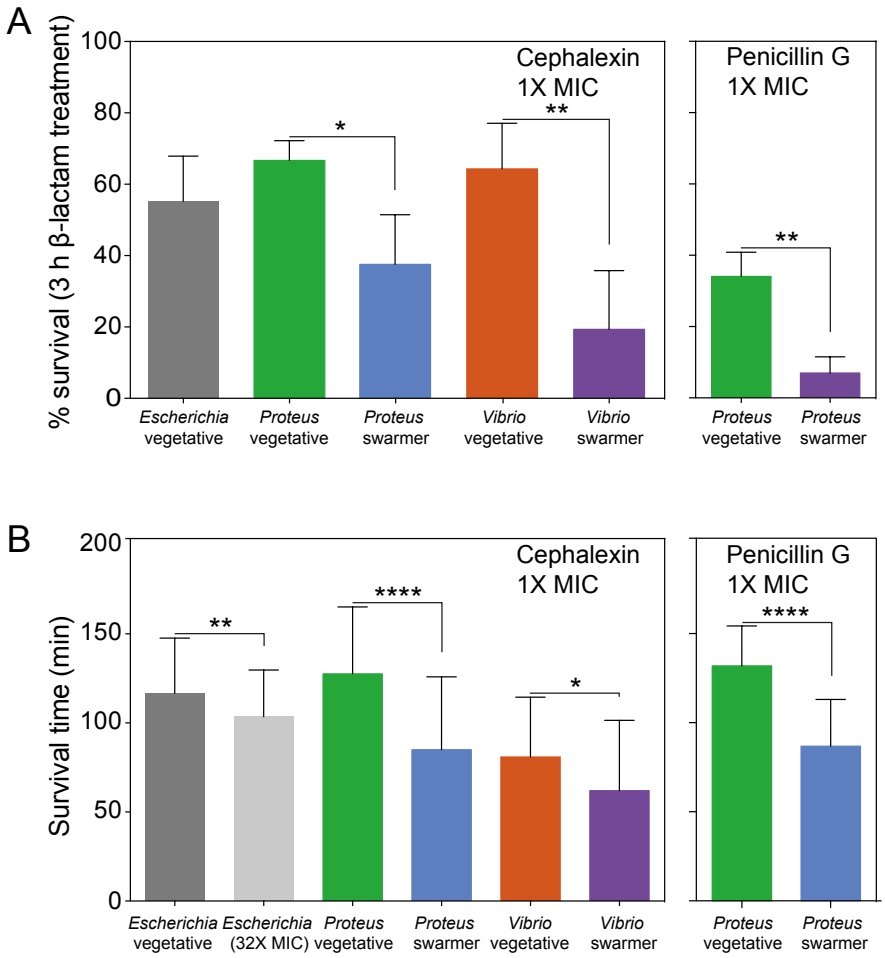

593

594 **Fig 7.**